Many-body potentials and dynamics based on diatomics-in-molecules: Vibrational frequency shifts in Ar_nHF ($n=1-12,62$) clusters

B. L. Grigorenko and A. V. Nemukhin
Department of Chemistry, Moscow State University, Moscow, 119899, Russian Federation

V. A. Apkarian
Department of Chemistry, University of California, Irvine, California 92717

(Received 26 May 1995; accepted 5 January 1996)

The conjecture that limited basis diatomics-in-molecules type potentials may serve as an accurate representation of many-body interactions is explored through molecular dynamics simulations of Ar_nHF ($n=1-12,62$). The important ingredient in the constructed potentials is the inclusion of ionic configurations of HF. Once the admixture between ionic and covalent configurations is calibrated by reference to an *ab initio* surface of the ArHF dimer, a single three-body potential energy surface is defined, and used in subsequent simulations of larger clusters. The vibrational frequencies of HF, which are computed from velocity–velocity autocorrelation functions, quantitatively reproduce the cluster size dependent redshifts. © *1996 American Institute of Physics.* [S0021-9606(96)01814-6]

I. INTRODUCTION

Simulations represent indispensable tools for exploring energetics and dynamics in condensed media, systems in which many-body interactions dominate. Perhaps the most compelling justification for the significant body of work on clusters and cryogenic matrices of rare gases is that they provide model systems in which many-body phenomena induced by nonbonded interactions can be investigated systematically. The most prevalent approach taken to date in simulations of such model systems has been classical molecular dynamics, relying on single surface, pairwise additive potentials.[1–3] This approach has proven to be adequate where qualitative effects are explored. However, quantitative treatments, even in systems as simple as a neat van der Waals crystal, invariably require the input of many-body interactions.[1] The same fact underscores the difficulty in quantitative predictions of perturbations, and in particular of vibrational frequency shifts of impurities isolated in rare gas matrices.[4–10] The situation is more severe in the case of open shell fragments, which is a requisite ingredient in systems of chemical significance. Here, even the qualitative picture is compromised when strictly additive potentials are used.[11–13] Clearly, explicit consideration of potentials does not arise where the full Schrodinger equation, including electronic degrees of freedom, is solved along with the calculations of the nuclear dynamics. While such methods have been introduced and implemented in some cases, even with projected advances in computer technologies they are likely to remain of limited applicability.[14] Exploration of approaches intermediate between these two extremes, is of obvious value. The framework of diatomics-in-molecules (DIM), which we explore in the present work, provides one such approach.[15,16]

The DIM method allows the systematic construction of potential energy manifolds based on input from diatomic fragments, which for most systems can be determined with a high level of accuracy.[15,16] Once the computationally (or experimentally) intensive task of determining diatomic electronic potentials is completed, the many-body electronic problem is reduced to matrix diagonalization. Given that the basis set is limited, the procedure can be carried out efficiently, and can therefore be incorporated in dynamical calculations. Due to the facts that the method obviates the need for global surfaces and yields sufficiently accurate energetics of electronic manifolds, the DIM approach remains attractive in gas phase reactive scattering calculations.[17] The same considerations apply in many-body dynamics, and the framework has already been utilized in this context. The method has been particularly useful in treating ionic systems, such as rare gas cluster ions,[18] and ionic surfaces arising from impurity charge transfer states in rare gas solids, including charge delocalization effects.[19] The latter parallels experience in smaller ionic systems, such as alkali hydoxides, in which a proper admixture between ionic and neutral states was shown to be necessary to predict structural properties.[20] Although limited to only neutral states, the DIM framework was used in the first treatment of photodissociation dynamics in rare gas solids that incorporated nonadiabatic effects.[21] The treatments of energetics and dynamics of open shell atoms in rare gas solids in which nonadditive potentials are used, are in effect DIM treatments with highly limited bases.[11–13,22] Finally, the DIM method has been applied to extended states, by calculating the band structure of rare gas solids.[23]

We describe a DIM-based procedure for calculations of vibrational shifts of HF in argon clusters. Our aim is to evaluate the ability of the method to handle many-body contributions in a quantitative manner. Through extensive experimentation and theoretical analysis, HF–Ar complexes are among the most thoroughly characterized. Based on high resolution spectra, Hutson constructed an empirical vibration dependent anisotropic intermolecular potential for Ar–HF, the so-called H6(4,3,2) potential.[24] The surface could reproduce and predict experimental spectra to within 0.1 cm^{-1}. Given the accuracy of this potential, and the accurately known Ar–Ar potential,[25] by analyzing spectra of Ar_2HF, Ernesti and Hutson were able to extract contributions due to

 0021-9606/96/104(14)/5510/7/$10.00

nonadditivity.[26] The largest such effect was identified as arising from the interaction of the molecular dipole with the exchange quadrupole of Ar_2.[26] Notwithstanding this consideration, using the H6(4,3,2) potential, Bacic *et al.* calculated spectral shifts in Ar_nHF ($n=1-14$) under the assumption of additivity.[27] They obtained nonmonotonic redshifts of the molecular vibrational frequency, first by classical calculations[27(a)] and later by five-dimensional quantum calculations.[27(b),27(c)] The results were in good agreement with extant experimental data on clusters,[28] which include clusters up to Ar_4–HF,[28(d)] and HF isolated in solid Ar.[8,29] They also showed that upon completion of the first solvation shell the computed spectral shift coincided with that observed in Ar matrices. The success of the simulated redshifts is in great part due to the H6(4,3,2) potential which incorporates the effect that upon vibrational excitation of HF from $v=0$ to $v=1$, the HF–Ar attraction increases.[24] Since the HF–Ar potential depends on the H–F distance, this surface should be regarded as a three-body potential. Tao and Klemperer performed accurate *ab initio* calculations of the same surface, by resorting to complete fourth order perturbation theory (MP4) and using basis sets containing bond functions.[30] The resulting potential energy surface, to which we refer to as TK herein, was in excellent agreement with that of Hutson.

The thorough knowledge of the Ar–HF potential energy surface, and the fact that a primitive pairwise additive atom–atom potential cannot reproduce matrix-induced vibrational redshifts,[7,10] render this system uniquely suitable for developing nonempirical constructs for many-body nonbonded interactions. Clearly, the unmatched accuracy of the empirical Hutson potential with its 22 adjustable parameters is not sought. But rather an approximate, yet quantitative, surface of a clear theoretical basis is sought. Further, to be useful in dynamics calculations of large systems, we hope that a relatively simple surface can be constructed. The DIM approach critically depends on the choice of the set of polyatomic basis functions, i.e., on the choice of the model. To reproduce the required features of the HF–Ar potential energy surface, it is clear that both ionic and neutral surfaces of HF should be included. We note that the ground state of HF is partly ionic—population analyses lead to electronic structures of the type $H^{+0.5}F^{-0.5}$—and therefore contains a significant admixture of the excited state ion-pair character. This admixture will depend on bond length, and should therefore be expected to play the major role in describing the vibrational dependence of interactions. Our strategy is therefore to retain a minimal such basis set, for simplicity, and to use a calibration from the *ab initio* surfaces, to maintain accuracy.

The organization of the rest of the paper is as follows. In Sec. II we succinctly describe the method and the basis functions to be used. In Sec. III we describe the diatomic fragment energetics. The DIM surfaces are then adjusted, as described in Sec. IV, to yield an analytical three-body function suitable for the simulations. The simulation results are described in Sec. V, followed by the concluding remarks in Sec. VI.

TABLE I. Composition of the polyatomic basis functions, Φ_i, in terms of atomic states.

i	Ar	H/H^+	F/F^-
1	^1S	^2S	^2P_x
2	^1S	^2S	^2P_z
3	^1S	^1S	^1S

II. DIATOMICS-IN-MOLECULES MODEL FOR THE Ar–H–F POTENTIAL ENERGY SURFACE

In the DIM method, the energies for the N-atomic system are obtained by diagonalization of the full Hamiltonian matrix $\mathbf{H}$ in the basis of polyatomic basis functions (PBF's) Φ_i. According to the central assumption of the method, the electrons may be assigned to definite nuclei, and the molecule is then treated as consisting of atoms or ions $a,b,c,\ldots$. The functions, Φ_i, are linear combinations of antisymmetrized products of wave functions of selected atomic states, such that the resulting molecular states have correct spin and space symmetries. The full Hamiltonian is written as the sum of diatomic and atomic terms

$$\mathbf{H}=\sum_a \sum_{b>a} \mathbf{H}^{(ab)}-(N-2)\sum_a \mathbf{H}^{(a)}. \tag{1}$$

Each fragment matrix $\mathbf{H}^{(a)}$ or $\mathbf{H}^{(ab)}$ is expressed via energies of the corresponding atomic (a) or diatomic (ab) fragments, and the functions Φ_i are transformed so that the PBFs describe definite states of a given pair of atoms as well as the states of the whole system. The transformation depends on the particular fragment and on the molecular geometry. Thus with an ab fragment, the original basis Φ is related to the new basis Φ_{ab} by

$$\Phi_{ab}=\mathbf{R}_a^{ab}\mathbf{R}_b^{ab}\mathbf{T}_{ab}\Phi. \tag{2}$$

Here, $\mathbf{R}_a^{ab}$ and $\mathbf{R}_b^{ab}$ are the rotation matrices that transform the atomic functions to define the orbital momentum projection along the ab direction, and $\mathbf{T}_{ab}$ is the matrix for transformation to the spin-coupling scheme that defines the spin state of the diatomic ab.

Within the neglect-of-overlap approximation, which is generally accepted in this theory, the fragment Hamiltonian matrix is expressed as

$$\mathbf{H}^{(ab)}=(\mathbf{T}_{ab})^*(\mathbf{R}_b^{ab})^*(\mathbf{R}_a^{ab})^*\mathbf{B}_{ab}^{-1}\mathbf{V}_{ab}\mathbf{B}_{ab}\mathbf{R}_a^{ab}\mathbf{R}_b^{ab}\mathbf{T}_{ab}, \tag{3}$$

where $\mathbf{B}_{ab}$ is the matrix that transforms the diatomic Hamiltonian, in the absence of all other atoms, to the diagonal form $\mathbf{V}_{ab}$. Unitary in neglecting the overlap, the matrix $\mathbf{B}_{ab}$ has nonzero off-diagonal elements only when the corresponding PBFs describe pair states of the same symmetry, while other atomic functions are nonorthogonal.

For the Ar–H–F ground state of the $^1A'$ symmetry, we assume a limited set of PBFs which are given in Table I. The notation is consistent with the arrangement illustrated in Fig. 1—with the F atom located at the origin, the H atom lying on the z axis, and with ψ representing the angle between F–H and F–Ar directions ($\psi=0$ when Ar is on the z axis).

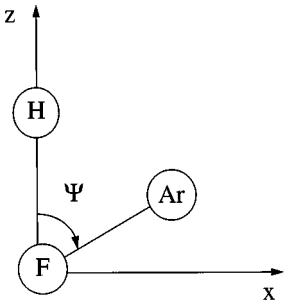

FIG. 1. Coordinate system used in the construction of the DIM matrices.

With the above choice of coordinates, the fragment Hamiltonian matrices are given as

$$\begin{aligned}
&\mathbf{H}^{(\mathrm{ArH})}=\mathbf{V}(\mathrm{ArH}),\\
&\mathbf{H}^{(\mathrm{ArF})}=(\mathbf{R}_{\mathrm{F}}^{\mathrm{HF}})^{*}\mathbf{V}(\mathrm{ArF})\mathbf{R}_{\mathrm{F}}^{\mathrm{HF}},\\
&\mathbf{H}^{(\mathrm{HF})}=\mathbf{B}_{\mathrm{HF}}^{-1}\mathbf{V}(\mathrm{HF})\mathbf{B}_{\mathrm{HF}},\\
&\mathbf{H}^{(\mathrm{Ar})}=\mathbf{V}(\mathrm{Ar}),\\
&\mathbf{H}^{(\mathrm{F})}=\mathbf{V}(\mathrm{F}),\\
&\mathbf{H}^{(\mathrm{H})}=\mathbf{V}(\mathrm{H}),
\end{aligned} \tag{4}$$

where all **V** matrices are diagonal, containing energies of the diatomic and atomic states

ii	11	22	33
$\mathbf{V}_{ii}(\ )$			
$\mathbf{V}_{ii}$(ArH)	$^2\Sigma$(ArH)	$^2\Sigma$(ArH)	$^1\Sigma(\mathrm{ArH}^+)$
$\mathbf{V}_{ii}$(ArF)	$^2\Pi$(ArF)	$^2\Sigma$(ArF)	$^1\Sigma(\mathrm{ArHF}^-)$
$\mathbf{V}_{ii}$(HF)	$^1\Pi$(HF)	$^1\Sigma$(HF)	$^1\Sigma(\mathrm{H}^+\mathrm{F}^-)$
$\mathbf{V}_{ii}$(Ar)	^1S(Ar)	^1S(Ar)	^{1}S(Ar)
$\mathbf{V}_{ii}$(F)	^2P(F)	^2P(F)	^{1}S(F^-)
$\mathbf{V}_{ii}$(**H**)	^2S(H)	^2S(H)	^{1}S(H^+)

(5)

The rotation matrix $\mathbf{R}_{\mathrm{F}}^{\mathrm{HF}}$ is now defined as

$$\mathbf{R}_{\mathrm{F}}^{\mathrm{HF}}=\begin{bmatrix}\cos(\psi) & \sin(\psi) & 0\\ -\sin(\psi) & \cos(\psi) & 0\\ 0 & 0 & 1\end{bmatrix}. \tag{6}$$

The matrix $\mathbf{B}_{\mathrm{HF}}$ is responsible for mixing the diatomic states of $^1\Sigma$ symmetry of HF which arise from the $\mathrm{H}(^2S)+\mathrm{F}(^2P)$ and $\mathrm{H}^+(^1S)+\mathrm{F}^-(^1S)$ dissociation limits. With the neglect of overlap, $\mathbf{B}_{\mathrm{HF}}$ may be expressed as

$$\mathbf{B}_{\mathrm{HF}}=\begin{bmatrix}1 & 0 & 0\\ 0 & \cos(\beta) & \sin(\beta)\\ 0 & -\sin(\beta) & \cos(\beta)\end{bmatrix} \tag{7}$$

in which the mixing parameter β depends on the H–F distance. For a given spatial configuration of the atoms, energies of the triatomic system, Ar–H–F are computed as the lowest eigenvalues of the 3×3 matrix

$$\mathbf{H}=\mathbf{H}^{(\mathrm{ArH})}+\mathbf{H}^{(\mathrm{ArF})}+\mathbf{H}^{(\mathrm{HF})}-\mathbf{H}^{(\mathrm{Ar})}-\mathbf{H}^{(\mathrm{F})}-\mathbf{H}^{(\mathrm{H})}. \tag{8}$$

III. FRAGMENT ENERGIES

All energies are referenced to the origin corresponding to the dissociation limit $\mathrm{Ar}(^1S)+\mathrm{H}(^2S)+\mathrm{F}(^2P)$. Based on the ionization potential of H and electron affinity of F, the dissociation limit of the ionic state, $\mathrm{H}^++\mathrm{F}^-$ is estimated as 0.373 30 hartree.[31] The required diatomic states, which we consider below, are those listed in Eq. (5). For the present application, HF energies restricted to the vicinity of the equilibrium distance $R_e(\mathrm{HF})=0.9169$ Å is needed. We consider the region between 0.85 and 1.1 Å, which approximately corresponds to vibrational excitations of HF up to $v=2$. A broader range of the potential curves for the ArH and ArF diatomic fragments is needed. Of particular importance are the regions 2–3 Å for the $\mathrm{ArH/ArH}^+$ fragment, and 3–4 Å for the $\mathrm{ArF/ArF}^-$ fragment. The reliability of surfaces is therefore tested in this range of configurations.

(1) HF ($X\,^1\Sigma$). A polynomial fit to the RKR data given in Ref. 32 was performed, and the dissociation energy, D_e, was taken from Ref. 33. The resulting function is given as (energies in hartrees, and distances in Å)

$$\begin{aligned}V(R)=&\,0.311\,027x^2-0.395\,204x^3+0.341\,791x^4\\&-0.258\,919x^5+0.126\,56x^6-D_e,\end{aligned} \tag{9}$$

where $x=R-0.9169$ and $D_e=0.2249$.

(2) HF($^1\Pi$). To create a potential curve for this repulsive state, *ab initio* calculations were carried out using the GAMESS package.[34] The configuration interaction (CI) procedure was applied with single and double excitations for the valence triple zeta basis set, augmented with two d-type functions on F and two p functions on H, [TZV+(2d,2p)]. In the range of internuclear distances of interest, 0.85 Å$<R<$1.1 Å, the potential energy is well represented by the fit

$$\begin{aligned}V(R)=&\,0.028\,41+0.170\,73\\&\times\exp(-(R-0.876\,1)/0.353\,94).\end{aligned} \tag{10}$$

(3) $H^+F^-(^1\Sigma)$. Energies of this ion-pair state were computed as second roots of the configuration interaction Hamiltonian matrix of Σ symmetry. Such computations are important for obtaining not only energies but also the mixing parameter, $\beta(R)$. The CI procedure with single, double, and triple excitations within the TZV+(2d,2p) orbital space was used. The potential curve referring to the second CI root corresponds to a bound state of a clear ionic character at long internuclear distances. Its minimum lies close to 2 Å, in accord with experimental estimates.[33] As measured from the $\mathrm{H}(^2S)+\mathrm{F}(^2P)$ limit, the computed points in the region 0.85 Å$<R<$1.1 Å are well represented by the function

$$\begin{aligned}V(R)=&\,0.203\,23+0.284\,73\\&\times\exp(-(R-0.686\,63)/0.231\,91).\end{aligned} \tag{11}$$

Ab initio values of the mixing parameter between ionic and covalent surfaces, $\beta(R)$ were generated by simulating a valence bond type wave function.[35] To this end, for each HF internuclear distance canonical molecular orbitals calculated with the TZV+(2d,2p) basis set were transformed to natural atomic orbitals,[36] which were subsequently used in the mul-

ticonfigurational expansion of the fully optimized reaction space (FORS) (or, equivalently, the complete active space). When two localized orbitals which mimic the fluorine ^2P and hydrogen ^1S orbitals are included in FORS for occupation by two electrons (all other orbitals kept doubly occupied) the relative weights of purely ionic and purely covalent contributions can be deduced, yielding an estimate of the mixing parameter $\beta(R)$. In the chosen region of HF distances, $\beta \sim 45°$ and nearly independent of R.

(4) ArH($^2\Sigma$). Effective potentials for the Ar–H interaction, commonly approximated by the Lennard-Jones form, have been widely used. However, since the range 2 Å$<R<$3 Å is crucial in the present application, and since this corresponds to the least reliably known repulsive wall of the potential, new *ab initio* calculations were carried out. The energies of ArH($^2\Sigma$) were computed by configuration interaction (CID) and perturbation theory (MP2) methods, using the recently developed effective core potential for Ar and the $[4s4p3d1f]$ basis set.[37] For hydrogen, the TZV $+(2d,2p)$ basis set was used. For distances 2 Å$<R$(ArH)$<$4 Å, the computed potential curve can be fitted with a single exponential

$$V(R) = 20.2 \exp(-3.414R). \tag{12}$$

(5) ArH^+($^1\Sigma$). This potential curve has been previously studied by various *ab initio* methods,[38(a)–38(d)] focusing mainly on the the region near the potential minimum, near R_e=1.28 Å. A proper breakdown of the ionic interactions in terms of induction and dispersion contributions is necessary for constructing the many-body surfaces, in this case the attractive wall in the range 2 Å$<R<$3 Å being the most important. For this purpose, the Morse parameterization given in Ref. 38(a) is not adequate, since it does not guarantee correct asymptotic behavior. Therefore, we recalculated the energies of this state using the same approaches as in the case of ArH.[33] We obtained reasonable estimates for the ArH^+ molecular parameters (R_e=1.282 Å, w_e=2593 cm^{-1}) which are consistent with both known experimental data[38(e)] (R_e=1.280 A, w_e=2710 cm^{-1}), and prior theoretical results.[38(a)–38(d)] Ignoring the region around the potential minimum, in the range 2 Å$<R$(ArH)$<$5 Å, the computed potential is well fit by the function

$$V(R) = -11.3017 \exp(-2.548R) - 0.4346/R^4 \tag{13}$$

in which the experimental polarizability of Ar, 11.1 a.u., has been used for the charge induced dipole term (the $c4$ term).

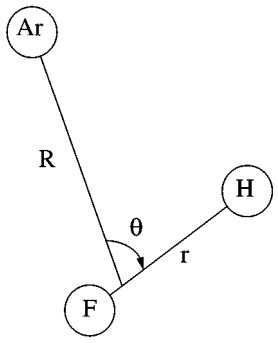

FIG. 2. Coordinate system used for description of the ArHF potential energy surface.

(6) ArF ($^2\Sigma$) and ArF ($^2\Pi$). The potential curves for these states have been extracted from experimental, atomic scattering, data.[39] We use the parametrizations cited in Ref. 39(a).

(7) ArF^-($^1\Sigma$). The results of combined *ab initio* calculations and semiempirical estimates for this potential have been described by Ahlrichs *et al.*[40] The analytical form given by them has a clear interpretation in terms of the electrostatic moments. We use it here in the form given therein.

IV. THE DIM POTENTIAL FOR ArHF

The DIM energies for the ground state of Ar–H–F were adjusted by comparison to the *ab initio* TK surface,[30] which, as mentioned earlier, is quite consistent with the empirical Hutson potential.[24] We discuss the comparisons using the coordinate system illustrated in Fig. 2; where R is the distance from Ar to the center of mass of HF, r is the H–F distance, θ is the angle between R and r directions. This coincides with the coordinate system used in the prior studies.[24,30]

The computed potential energy surface, without any adjustment parameters, qualitatively reproduces the features of the TK surface. In particular, it predicts the proper global minimum and the sign of the vibrational shift upon clustering, i.e., as the bond length of HF is increased, the attraction between Ar and HF is increased. However, the computed interaction energies fail badly. For instance, at the linear equilibrium geometry, θ=0, R=3.5 Å, r=0.9169 Å, the computed DIM interaction energy is 2000 cm^{-1} while the

TABLE II. Angle dependences (see Fig. 2) of characteristic parameters of the ArHF potential: Positions, R_m (in Å), and depths, V_m (in cm^{-1}), of the potential well and the energy differences $V_m(\theta=0)-V_m(\theta)$ obtained in the present work, in the MP4 calculations of Tao and Klemperer (Ref. 30) and in the spectroscopic parametrization of Hutson (Ref. 24).

	$R_m(\theta)$			$V_m(\theta)$			$V_m(0)-V_m(\theta)$	
Method	0	90	180	0	90	180	90	180
Present	3.53	3.48	3.27	218	87	122	131	96
Ref. 30	3.47	3.555	3.43	202	73	90	130	113
Ref. 24	3.434	3.496	3.375	220	83	108	137	113

TABLE III. HF frequency shifts in Ar_nHF clusters as a function of cluster size n.

	$\Delta\nu$ (cm^{-1})			
	Experiment		Theory	
n	Ref. 28	Present	Ref. 27(a)	Ref. 27(c)
1	−9.654	−10	−19	−10
2	−14.827	−20	−23	−16
3	−19.260	−30	−29	−21
4	−19.697	−30	−28	−22
5		−34	−29	−22
6		−32	−29	−25
7		−33	−30	−26
8		−34	−30	−26
9		−36	−35	−37
10		−37	−36	−39
11		−37	−40	−40
12		−38	−45	−43
62		−40		
Matrix[a]	−41			

[a]From Ref. 8.

expected value is 200 cm^{-1}. This disagreement can be attributed to the overestimate of the binding in the ionic surface by the pairwise treatment of ArH^+ and ArF^- potentials, which we correct below by adding a three-body term; and due to the overestimate of the *ab initio* mixing coefficient, β, which in turn is probably the result of the limited basis set used. Upon adjusting β to reproduce the potential energy minimum, a nearly quantitative agreement with the TK surface results.

In the limited range of relevance to calculations of spectral shifts, upon numerical and analytical analysis of the DIM surfaces, a further simplification is realized. Namely, the Ar–H–F surface can be generated by an analytic formula (with angle ψ defined in Fig. 1)

$$V(\mathrm{ArHF}) = V(\mathrm{HF},\Sigma) + [V(\mathrm{ArF},\Sigma)\cos^2(\psi) + V(\mathrm{ArF},\Pi)\sin^2(\psi) + V(\mathrm{ArH})]\cos^2(\beta) + [V(\mathrm{ArF}^-) + V(\mathrm{ArH}^+)]\sin^2(\beta). \quad (14)$$

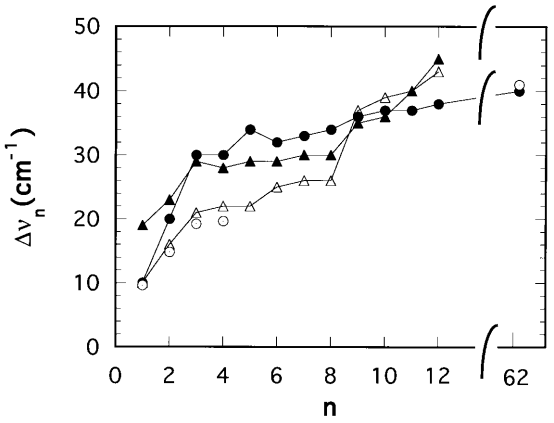

FIG. 3. HF vibrational shifts of Ar_nHF as a function of n: (○) experimental data of Ref. 28, the last point is from the matrix shift from Ref. 8; (●) present results; (▲) theory with classical treatment of vibrations, Ref. 27(a); (△) theory with quantum treatment of vibrations, Ref. 27(c).

This formula may be derived by expanding the true DIM expressions for the lowest energy surface near leading terms at particular geometries (ψ=0, $\psi=\pi$, or $\psi=\pi/2$). Comparison of the numbers obtained by Eq. (14) with those generated by diagonalization of the Hamiltonian, Eq. (8), showed that the energies differed by no more than 20 cm^{-1}.

The expression of Eq. (14) is quite transparent. By definition, β is responsible for mixing neutral and ionic states in this system. In the absence of mixing, when β is set to 0 in Eq. (14), the pairwise approximation for the triatomic potential energy is obtained. If, further, the anisotropy of the Ar–F potential were to be neglected by assuming an effective Ar–F potential (e.g., as given in Ref. 5), then the simple pairwise approximation is retrieved

$$V(\mathrm{ArHF}) = V(\mathrm{HF}) + V(\mathrm{ArF}) + V(\mathrm{ArH}). \quad (15)$$

We note, once more, that Eq. (15) cannot predict the observed vibrational redshifts. For $\beta\neq0$ in Eq. (14), mixing between ionic and covalent surfaces occurs, leading to the correct topology of the three-body surface.

While application of an analytic formula, instead of solving the original DIM secular equation, introduces a further approximation; given its simplicity and computation economy, we use it in the calculations of spectral shifts. To this end, the DIM surface of Eq. (14) was further refined by adjusting $\beta(r)$ using the TK surface as reference, and the observed vibrational shift of HF as the target. Noting that the attrative potentials of the ionic interactions, ArH^+ and ArF^- are dominated by nonadditive induction terms, with the leading term being the $c4/R^4$ charge-induced-dipole term, we separate this term into a three-body contribution in the ionic $Ar–H^+F^-$ surface[41]

$$V_{\mathrm{ion}} = \frac{\alpha(\mathrm{Ar})\cos\varphi}{R_{\mathrm{ArH}}^2 R_{\mathrm{ArF}}^2}, \quad (16)$$

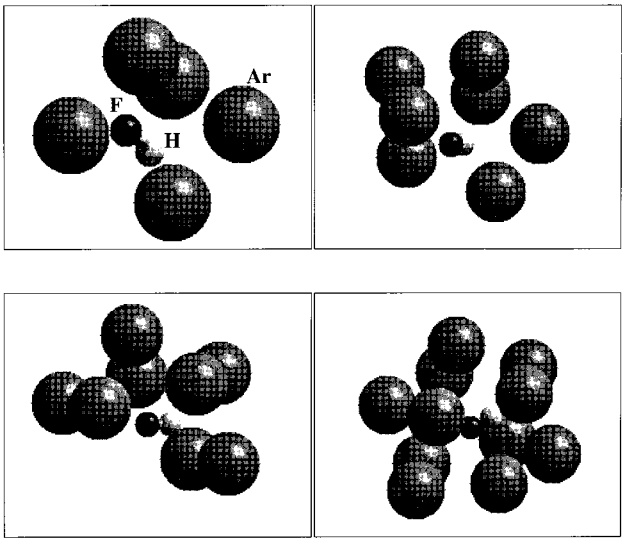

FIG. 4. The minimum energy structures for Ar_nHF. Only structures, n=5,7,8,11, which differ from those found in Ref. 27 are shown.

where α(Ar) is the polarizability of Ar, and ϕ is the angle between the vectors R_{ArH} and R_{ArF}. Finally, with a choice of the mixing parameter in the form

$$\beta(r)=20.3+5r \tag{17}$$

in which β given in degrees, and r is in Å, a surface in reasonable agreement with both the TK as well as the Hutson surface results. A comparison of some of the characteristic points of the surface is presented in Table II (which may be compared to Table VII of the TK paper[30]). Within the parameter range used in our adjustment, a better fit to the reference surfaces could be obtained.

However, that could only be achieved by sacrificing the accuracy of the predicted spectral shifts. The latter we had chosen as a more crucial criterion to satisfy.

V. VIBRATIONAL SHIFTS IN AR(n)HF CLUSTERS

With the above construct of the Ar–H–F potential, classical molecular dynamics calculations for the Ar_nHF clusters ($n=0,1–12,62$) were performed. The Aziz–Chen potential parameters were used to describe the Ar–Ar interactions.[25] The potential for Ar_nHF was computed according to

$$V(n)=\sum_i V[\mathrm{Ar}_i\mathrm{HF}(R_i,\theta_i,r)]+\sum_{i<j} V[\mathrm{Ar}_i\mathrm{Ar}_j(R_{ij})], \tag{18}$$

where indices i and j run over Ar atoms, R_i is the distance from Ar_i to the HF center of mass, and θ_i is the angle between R_i and the HF bond. In effect, contributions from each triangle Ar–H–F is computed with the DIM-based potential of Eq. (14). The steepest descent method was used to locate stationary points on respective potential energy surfaces. After geometry relaxation leading to minimum energy configurations, the systems were allowed to evolve at temperatures close to zero. The equations of motion were integrated using the Gear algorithm with a time step of 5×10^{-16} s. After equilibration, trajectories consisting of 10^4 steps were propagated to generate the velocity–velocity autocorrelations.

The HF vibrational frequencies, computed from the power spectrum of the velocity–velocity autocorrelation functions, are collected in Table III and illustrated in Fig. 3. The nonmonotonic shifts generally track those of Basic *et al.*,[27] which are based on the empirical Hutson potential.[24] The calculated shifts in the present show a reasonable agreement with the existing experimental data,[28(d)] along with the saturation effect which corresponds to the vibrational shift observed in Ar matrices.[8,29] In the case of Ar_nHF ($n=2,3,4$) the agreement of our results with experiment is poorer. This is can be traced to the approximation made by the classical dynamics used in the present calculation of frequencies, as opposed to the potential surface. Indeed, it is the multidimensional quantum treatment of vibrations by Bacic *et al.*[27(c)] that produced nearly exact agreement with experiment, while their earlier calculations of the shifts,[27(a)] produced results that are nearly identical to the present (see comparisons in Table III).

The lowest energy cluster geometries found in our work generally agree with those presented in Ref. 27(a). The pictures for clusters Ar(n)HF with $n=1,2,3,4,6,9,12$ seem to be the same as those shown there. For clusters with $n=5,7,8,11$, our procedure yielded different lowest energy configurations. The new structures for these clusters are illustrated in Fig. 4. In all cases we have detected the configurations pictured for these clusters in Ref. 27(a), however, in our calculations their energies are higher (by 10–35 cm^{-1}) than for the structures shown in Fig. 4.

VI. CONCLUSIONS

We have constructed a diatomics-in-molecules type potential energy surface for the Ar–HF dimer, with a minimal basis set that includes ionic and covalent states of HF. The primitive surface, without any adjustments, has the proper topology: It predicts a redshift for the HF vibration upon clustering with Ar. With adjustments of pair potential parameters within acceptable bounds, and upon calibrating the mixing parameter between ionic and neutral states, the surface is capable of reproducing the main features of the *ab initio* potential energy surface of Tao and Klemperer,[30] and the empirical potential of Hutson.[24] Without further adjustments, the vibrational redshift of HF in Ar_nHF ($n=1–12$) is reproduced, in agreement with calculations based on the empirical surfaces.[27] Thus the present results reinforce those already established in regards the solvation of HF in Ar clusters.

For clusters with $n=5,7,8,11$ our procedure resulted in lowest energy configurations different from those obtained in Ref. 27(a). A variety of isomeric structures on the shallow potential energy surfaces obviously complicates a search of minimum energy points for these systems.

The main conclusion of these results is that the DIM model, with a proper mixing of neutral and ionic states, provides a reasonable representation of the three-body Ar–H–F surface.

Unlike the empirical potentials the present surface is not of a spectroscopic accuracy. However, it is an economical representation with sufficient accuracy to be well suited for simulations in large systems. Moreover, the formulation provides direct insights into the origin of the sources of nonadditivity of interactions. In the present application, where only a limited range of the surface is of relevance, we have further simplified the potential by using an analytical form. More generally, by solving the secular equations at each step of the numerical integration of equations of motion, this approach can be used for dynamical computations where nonstationary points, far from equilibrium configurations are required. Such applications are presently underway.

ACKNOWLEDGMENTS

This research was supported in part by the Russian Basic Research Foundation (Grant No. 95-03-08205), International Science Foundation and Russian Government (Grant No. MHo300), and the U.S. Air Force Office of Scientific Research (Grant No. F49620-95-0213).

[1] (a) *Inert Gases*, edited by M. L. Klein (Springer, New York, 1984); (b) M. L. Klein, Chem. Rev. **90**, 459 (1990).
[2] R. M. Whitnell and K. R. Wilson, *Reviews of Computational Chemistry*, edited by K. B. Lipkowitz and D. B. Boyd (VCH, New York, 1994), Vol. IV, pp. 67–184.
[3] R. B. Gerber, A. B. McCoy, and A. Garcia Vela, Annu. Rev. Phys. Chem. **45**, 275 (1994).
[4] (a) R. Gunde, P. Felder, and H. H. Gunthard, Chem. Phys. **64**, 313 (1982); (b) R. Gunde, H. J. Keller, T.-K. Ha, and H. H. Gunthard, J. Phys. Chem. **95**, 2802 (1991).
[5] L. M. Raff, J. Chem. Phys. **95**, 8901 (1991).
[6] (a) M. Winter, K. Seranski, and U. Schurath, Chem. Phys. **159**, 235 (1992); (b) K. Seranski, M. Winter, and U. Schurath, *ibid*. **159**, 247 (1992).
[7] (a) R. Fraenkel and Y. Haas, J. Chem. Phys. **100**, 4324 (1994); (b) R. Fraenkel and Y. Haas, Chem. Phys. Lett. **220**, 7 (1994); (c) R. Fraenkel and Y. Haas, Chem. Phys. **186**, 185 (1994).
[8] D. T. Anderson and J. S. Winn, Chem. Phys. **189**, 171 (1994).
[9] (a) A. V. Nemukhin, B. L. Grigorenko, and G. B. Sergeev, Can. J. Phys. **72**, 909 (1994); (b) B. L. Grigorenko, A. V. Nemukhin, G. B. Sergeev, V. S. Stepanyuk, and A. Szasz, Phys. Rev. B **50**, 18666 (1994); (c) A. V. Nemukhin and B. L. Grigorenko, Chem. Phys. Lett. **223**, 627 (1995).
[10] A. I. Krylova, A. V. Nemukhin, and N. F. Stepanov, J. Mol. Struct. (THEOCHEM) **262**, 55 (1992).
[11] M. E. Fajardo, J. Chem. Phys. **98**, 119 (1993).
[12] (a) W. G. Lawrence and V. A. Apkarian, J. Chem. Phys. **101**, 1820 (1993); (b) A. V. Danilychev and V. A. Apkarian, *ibid*. **100**, 5556 (1994); (c) K. Kizer and V. A. Apkarian, *ibid*. **103**, 4945 (1995).
[13] (a) A. I. Krylov, and R. B. Gerber, J. Chem. Phys. **100**, 4242 (1994); (b) A. I. Krylov, R. B. Gerber, and V. A. Apkarian, Chem. Phys. **189**, 261 (1994).
[14] (a) R. Car and M. Parrinello, Phys. Rev. Lett. **55**, 2471 (1985) (b) S. A. Maluendes and M. Dupuis, Int. J. Quantum Chem. **42**, 1327 (1992).
[15] F. O. Ellison, J. Am. Chem. Soc. **85**, 3540 (1963).
[16] J. C. Tully, in *Modern Theoretical Chemistry*, Semiempirical Methods of Electronic Structure Calculation, Vol. 7A, edited by G. A. Segal (Plenum, New York, 1977), Chap. 6.
[17] P. J. Kuntz, *Atom–Molecule Collision Theory—A Guide for the Experimentalist*, edited by R. B. Bernstein (Plenum, New York, 1979), Chap. 3, p. 79.
[18] M. Fieber, A. Ding, and P. J. Kuntz, Z. Phys. D **23**, 171 (1992).
[19] (a) I. Last and T. F. George, J. Chem. Phys. **87**, 1183 (1987); (b) I. Last, T. F. George, M. E. Fajardo, and V. A. Apkarian, *ibid*. **87**, 5917 (1987); (c) I. Last and T. F. George, *ibid*. **98**, 6406 (1993).
[20] (a) A. V. Nemukhin and N. F. Stepanov, Int. J. Quantum Chem. **15**, 49 (1979); (b) J. Mol. Struct. **67**, 81 (1980); (c) Chem. Phys. Lett. **63**, 396 (1979); (d) A. V. Zaitsevskii, A. V. Nemukhin, and N. F. Stepanov, Int. J. Quantum Chem. **17**, 679 (1980); (e) S. V. Ljudkovskii, A. V. Nemukhin, and N. F. Stepanov, J. Mol. Struct. (Theochem) **104**, 403 (1983).
[21] I. H. Gersonde, S. Hennig, and H. Gabriel, J. Chem. Phys. **101**, 9558 (1994); I. H. Gersonde and H. Gabriel, *ibid*. **98**, 2094 (1993).
[22] L. C. Balling and J. J. Wright, J. Chem. Phys. **79**, 2941 (1983).
[23] H. H. Vongrunberg, I. H. Gersonde, and H. Gabriel, Zeits. Phys. D **28**, 145 (1993).
[24] J. Hutson, J. Chem. Phys. **96**, 6752 (1992).
[25] R. A. Aziz and H. H. Chen, J. Chem. Phys. **67**, 5719 (1977).
[26] A. Ernesti and J. M. Hutson, Phys. Rev. A **51**, 239 (1995).
[27] (a) S. Liu, Z. Bacic, J. W. Moskowitz, and K. E. Schmidt, J. Chem. Phys. **100**, 7166 (1994); (b) **101**, 6359 (1994); (c) **101**, 10181 (1994).
[28] (a) H. S. Gutowsky, T. D. Klots, C. Chuang, C. A. Schmuttenmaer, and T. Emilsson, J. Chem. Phys. **86**, 569 (1987); (b) H. S. Gutowsky, T. D. Klots, C. Chuang, J. N. Keen, C. A. Schmuttenmaer, and T. Emilsson, J. Am. Chem. Soc. **109**, 5653 (1987); (c) H. S. Gutowsky, C. Chuang, T. D. Klots, T. Emilsson, R. S. Ruoff, and K. P. Krause, J. Chem. Phys. **88**, 2919 (1988); (d) A. McIlroy, R. Lascola, C. M. Lovejoy, and D. J. Nesbitt, J. Phys. Chem. **95**, 2636 (1991).
[29] (a) M. T. Bowers, G. I. Kerley, and W. H. Flygare, J. Chem. Phys. **45**, 3399 (1966); (b) M. G. Mason, W. G. Von Holle, and D. W. Robinson, *ibid*. **54**, 3491 (1971); (c) L. Andrews and G. L. Johnson, Chem. Phys. Lett. **96**, 133 (1983); (d) L. Andrews and G. L. Johnson, J. Phys. Chem. **88**, 425 (1984); (e) R. L. Redington and D. F. Hamill, J. Chem. Phys. **80**, 2446 (1984).
[30] F. M. Tao and W. Klemperer, J. Chem. Phys. **101**, 1129 (1994).
[31] M. I. Boulos, P. Fauchais, and E. Pfender, *Thermal Plasmas. Fundamentals and Applications* (Plenum, New York, 1994), Vol. 1, p. 452.
[32] D. Schwenke, and D. Truhlar, J. Chem. Phys. **88**, 4800 (1988).
[33] K. P. Huber and G. Herzberg, *Molecular Spectra and Molecular Structure. IV. Constants of Diatomic Molecules* (Van Nostrand Reinhold, New York, 1979).
[34] M. W. Schmidt, K. K. Baldridge, J. A. Boatz, J. H. Jensen, S. Koseki, M. S. Gordon, K. A. Nguyen, T. L. Windus, and S. T. Elbert, Quantum Chem. Program Exchange Bull. **1990**, 52.
[35] A. V. Nemukhin and F. Weinhold, J. Chem. Phys. **97**, 1095 (1992).
[36] F. Weinhold and J. E. Carpenter, in *The Structure of Small Molecules and Ions*, edited by R. Naaman and Z. Vager (Plenum, New York, 1988), p. 227.
[37] A. Nicklass, M. Dolg, H. Stoll, and H. Preuss, J. Chem. Phys. **102**, 8942 (1995).
[38] (a) F. A. Gianturco and M. Patriarca, Nuovo Cimento D **11**, 1287 (1989); (b) M. E. Rosenkrantz, Chem. Phys. Lett. **173**, 378 (1990); (c) P. Rosmus, Theoret. Chim. Acta **51**, 359 (1979); (d) J. Lundell, J. Nieminen, and H. Kunttu, Chem. Phys. Lett. **208**, 247 (1993); (e) J. W. C. Johns, J. Mol. Spectrosc. **106**, 124 (1984).
[39] (a) V. Aquilanti, E. Luzzatti, F. Pirani, and G. G. Volpi, J. Chem. Phys. **89**, 6165 (1988); (b) C. H. Becker, P. Casavecchia, and Y. T. Lee, *ibid*. **70**, 2986 (1979).
[40] R. Ahlrichs, H. J. Bohm, S. Brode, K. T. Tang, and J. P. Toennies, J. Chem. Phys. **88**, 6290 (1988).
[41] I. Last and T. F. George, J. Chem. Phys. **86**, 3787 (1987); Chem. Phys. Lett. **183**, 547 (1991).